Science of the Total Environment 896 (2023) 165266

Contents lists available at ScienceDirect

Science of the Total Environment

journal homepage: www.elsevier.com/locate/scitotenv

Historical disconnection from floodplain alters riparian forest composition, tree growth and deadwood amount

J. Julio Camarero [a,*], Michele Colangelo [a,b], Patricia M. Rodríguez-Gonzalez [c]

[a] Pyrenean Institute of Ecology (IPE-CSIC), Avda. Montañana 1005, 50192 Zaragoza, Spain
[b] School of Agricultural, Forestry, Food and Environmental Sciences, University of Basilicata, Viale dell'Ateneo Lucano 10, 85100 Potenza, Italy
[c] Forest Research Centre and Associate Laboratory TERRA, School of Agriculture, University of Lisbon, Lisbon 1349-017, Portugal

HIGHLIGHTS

- River sinuosity in the middle Ebro basin declined from 1927 to 2015.
- Sinuosity loss leads to forests dominated by less phreatophytic tree species.
- Disconnection from floodplain increased the amount of decayed deadwood.
- River flow diversion reduced tree growth and increased vulnerability to drought.

GRAPHICAL ABSTRACT

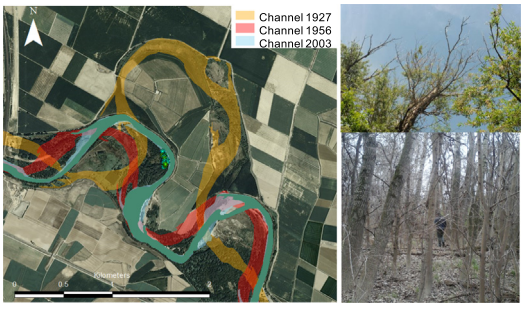

Riparian forest dynamics are altered by human modification of river geomorphology (loss of sinuosity) leading to dieback

ARTICLE INFO

Editor: Manuel Esteban Lucas-Borja

Keywords:
Deadwood
Dendroecology
Floodplain forest
River flow
Sinuosity

ABSTRACT

Riparian forests are among the most dynamic but threatened terrestrial ecosystems. Their dynamism and conservation depend on historical changes in river geomorphology, which can be evaluated through changes in channel sinuosity. However, we lack long-term assessments on sinuosity and how they impact riparian forest composition, tree growth and deadwood amount. To fill this research gap, we reconstructed river sinuosity in 14 sites across the middle Ebro basin, north-eastern Spain, using historical aerial photographs taken in 1927, 1956, 1998–2003 and 2014–2015. Relationships between sinuosity, stand composition and deadwood amount and decay degree were calculated. We also reconstructed radial growth of the major tree species (*Populus alba*, *Populus nigra*, *Fraxinus angustifolia*, *Salix alba* and *Ulmus minor*) in two sites to evaluate how coupled it was with changes in river flow after dam building. From 1927 to 2015, sinuosity decreased passing from 1.39 to 1.20. The river dynamics were altered in the 1950s and 1960s after dam and dyke building. Sites with high sinuosity values in 1956 corresponded to mature stands with large *P. nigra* individuals. Sinuosity was negatively related to *F. angustifolia* ($r_s = -0.83$, $p < 0.001$) and *P. alba* ($r_s = -0.64$, $p = 0.02$) abundance, whereas sites dominated by *P. alba* and *U. minor* presented abundant decayed deadwood. A loss of sinuosity and a contraction of the riverbank gradient increased disconnection of active channel from floodplain, with a mixing of more (e.g., *P. nigra*) and less phreatophytic species (e.g., *U. minor*). River flow diversion reduced growth and increased the tree-to-tree *P. alba* growth coherence. Hydrological droughts contributed to growth decline and dieback of *U. minor*, which is sensitive to spring river flow. Conservation and restoration of riparian forests must consider historical changes in river geomorphology related to human activities.

* Corresponding author.
E-mail addresses: jjcamarero@ipe.csic.es (J.J. Camarero), michele.colangelo@unibas.it (M. Colangelo), patri@isa.ulisboa.pt (P.M. Rodríguez-Gonzalez).

http://dx.doi.org/10.1016/j.scitotenv.2023.165266
Received 5 May 2023; Received in revised form 30 June 2023; Accepted 30 June 2023
Available online 03 July 2023

1. Introduction

Riparian forests are highly dynamic and diverse ecosystems where trees act as ecosystem engineers (Gurnell, 2014). Ecohydrology studies have shown how these forests interact with river dynamics increasing geomorphological complexity (Piégay and Gurnell, 1997; Gurnell et al., 2002; Montgomery et al., 2003), thus representing major sources of deadwood (Sear et al., 2010; Polvi and Wohl, 2013). Therefore, these forests play key roles in riverine ecological processes (Ferreira et al., 2018). Riparian forests provide several ecosystem services in addition to increasing productivity. They also trap fine sediments, remove nutrients from runoff, regulate water temperature and radiation, increase bank stability and reduce the erosive power of the channel (Manga and Kirchner, 2000). The acknowledgment of the benefits provided by these forests has triggered restoration and conservation programs to mitigate and manage flood risk, yet often with limited success (Cortina-Segarra et al., 2021). However, to improve the stability of such restoration initiatives, long-term historical and integrative approaches are required (Broadmeadow and Nisbet, 2004; Lane, 2017; Nilsson et al., 2018).

The high dynamism and hydro-dependence of riparian forests makes them responsive to changes in hydrologic regimes (e.g., river regulation, groundwater depletion) and changes in land use and climate extremes (e.g., droughts, heat waves) at different spatial and temporal scales (Rodríguez-González et al., 2010; Stella and Bendix, 2019; Havrdová et al., 2023). So, we need multi-scale approaches to assess those responses considering long-term river-forest interactions (Gurnell et al., 2020). For instance, the different amounts and decay degrees of deadwood positively influence biodiversity in riparian forests, but tree growth and deadwood accumulation are long-term processes whose assessment requires retrospective approaches (Collins et al., 2002). According to growth models, it can take 20–40 years after stand establishment to deliver enough in-channel deadwood, whilst at least 100 years are needed until abundant channel deadwood allows mitigating flood impacts (Dixon et al., 2019).

The amount and decay of deadwood in riparian forests results from river-forest dynamics (Ruiz-Villanueva et al., 2016). Deadwood affects forest carbon and nutrient fluxes and it is a biodiversity hub for saproxylic species (Holmes et al., 2010; Pollock and Beechie, 2014). The volume and decay degree of deadwood in riparian forests depend on several factors including bedrock and soil type, continuous inputs from uplands and floodplain, episodic disturbances (floods, storms) and climate conditions (Le Lay et al., 2013). For instance, wood decay rates are faster in more humid and warmer riparian forests than in drier and colder mountain forests (Charles et al., 2022; Oettel et al., 2022).

River regulation (e.g., through dam or dyke building) and climatic drought lower soil water availability and can trigger the decline of some riparian forests impairing some of their ecosystem services such as carbon uptake or deadwood production (Williams and Cooper, 2005). Furthermore, persistent declines of shallow groundwater coupled with human-induced channel disconnection from floodplain can reduce riparian forest cover negative impacting long-term growth and deadwood production, particularly in low floodplain terraces and semiarid regions (Stromberg et al., 1996). Therefore, historical reconstructions of river dynamics and tree growth combined with field assessments of the lying deadwood amount are essential to understand long-term developmental processes in riparian forests (e.g., changes in growth and deadwood type). These data are demanded by managers to refine successional models and improve restoration and conservation of these menaced habitats.

We hypothesize that the sinuosity index has decreased from 1927 to 2015, as river dynamics was increasingly regulated through dam and dyke building, leading to an accumulation of less-decayed deadwood and promoting the shift of riparian forests composition towards non-phreatophytic species such as *F. angustifolia* and *U. minor*. Negative impacts of hydrological and climatic droughts in combination with Dutch elm disease, caused by the fungus *Ophiostoma novo-ulmi* Brasier, are expected to negatively impact radial growth and vigor of *U. minor*. Further, we also expect that flow diversion through river regulation would negatively impact growth and make it more similar by increasing tree-to-tree coherence, particularly in the case of phreatophytic cottonwoods (*Populus* spp.), which mainly use groundwater and are more coupled to changes in streamflow and water table depth than non-phreatophytes.

In this study we reconstructed river dynamics, using a river sinuosity index, across the middle Ebro basin (north-eastern Spain) by comparing historical aerial photographs taken in several periods (1927, 1956, 1998–2003 and 2014–2015) and related the sinuosity index to: (i) the amount and decay degree of lying deadwood, (ii) tree abundance, and (iii) changes in radial growth and its response to river flow variability of the main tree species (*Populus alba*, *Populus nigra*, *Fraxinus angustifolia*, *Salix alba* and *Ulmus minor*). The first two objectives were fulfilled in fourteen study sites distributed across the middle Ebro basin. The third objective was carried out in two more intensively studied forests which were located near Tudela and Zaragoza cities, at the NW and SE distribution limits of the study area.

The significance and novelty of this study rely on contextualizing long-term river-forest interactions by comparing historical aerial photographs, tree growth series and stand structural data including deadwood amount and decay degree. The analyses of these factors allow pinpointing human alterations of river geomorphology and evaluating their impacts on riparian forests.

2. Material and methods

2.1. Study sites

The study sites are well-structured, mature riparian forests ("soto" in Spanish) located in the Middle Ebro basin, north-eastern Spain (Fig. 1, Table 1). Some are located near Alfaro, Tudela and Zaragoza cities. The Ebro basin occupies 85,362 km^2 and it is the largest basin of the Mediterranean basin. In this region, the Ebro river has a low longitudinal slope and forms meandering channels (Ollero, 1990, 2007). The Ebro river was regulated through the building of dams and dikes in the 1950s and 1960s (Frutos et al., 2004), and this affected the recent dynamics of the study sites, particularly near Zaragoza city (e.g., Soto de Partinchas). In contrast, forests located near Alfaro (e.g., Soto de la Duquesa) and Tudela (e.g., Soto de la Remonta) show free-flowing river dynamics (Ayerra, 1988). River flow peaks from January to April (Fig. S1), but river regulation reduced winter flows and partially alleviated the low water levels in summer after the 1950s (Frutos et al., 2004). According to river flow data obtained from a gauging station located at 14 km from Tudela (Castejón, 1° 41′ W, 42° 11′ N, 260 m a.s.l.; period 1970–2018) the average annual discharge of the Ebro river registered was 7177 hm^3 and the contributing area of the catchment upstream the gauged station was 25,194 km^2. Near Zaragoza, the water table depth showed maximum values from October to April and minimum values from May to September (Camarero et al., 2023). Recent periods with very low (mean – 1.96 SD, where SD is the standard deviation) river flow values from winter to spring were: 1988–1990, 2001–2002, 2011–2012 and 2016–2017 (Fig. S2a).

Climate in the study area is Mediterranean with annual precipitation ranging 350–470 mm. The coldest and warmest months are January (5.4–5.6 °C) and July (22.7–23.6 °C), respectively. The summer dry period lasts from June to September. According to monthly climate data from the 0.5°-gridded CRU ver. 4.05 dataset (Harris et al., 2020) considering the period 1927–2015, mean temperature has increased ($\tau = 0.50$, $p < 0.001$), particularly after the 1970s, in the study area (1° 45′–0° 32′ W, 41° 29′–42° 22′ N), whereas total precipitation has significantly decreased ($\tau = -0.17$, $p = 0.02$) (Fig. S2b). In this region, marl and gypsum Miocene deposits are abundant leading to the formation of basic, loamy-sandy soils.

The study riparian forests are dominated by tamarisks (*Tamarix* spp., Fernández-González et al., 1990), white willow (*Salix alba* L.) and black poplar (*Populus nigra* L.) situated near the river bank, silver poplar (*Populus alba* L.) located in the transition zone, and narrow-leaved ash (*Fraxinus angustifolia* Vahl.) with scattered elm trees (*Ulmus minor* Mill.) located inland (Figs. S3, S4, S5, S6 and S7). Mature elms are often affected by

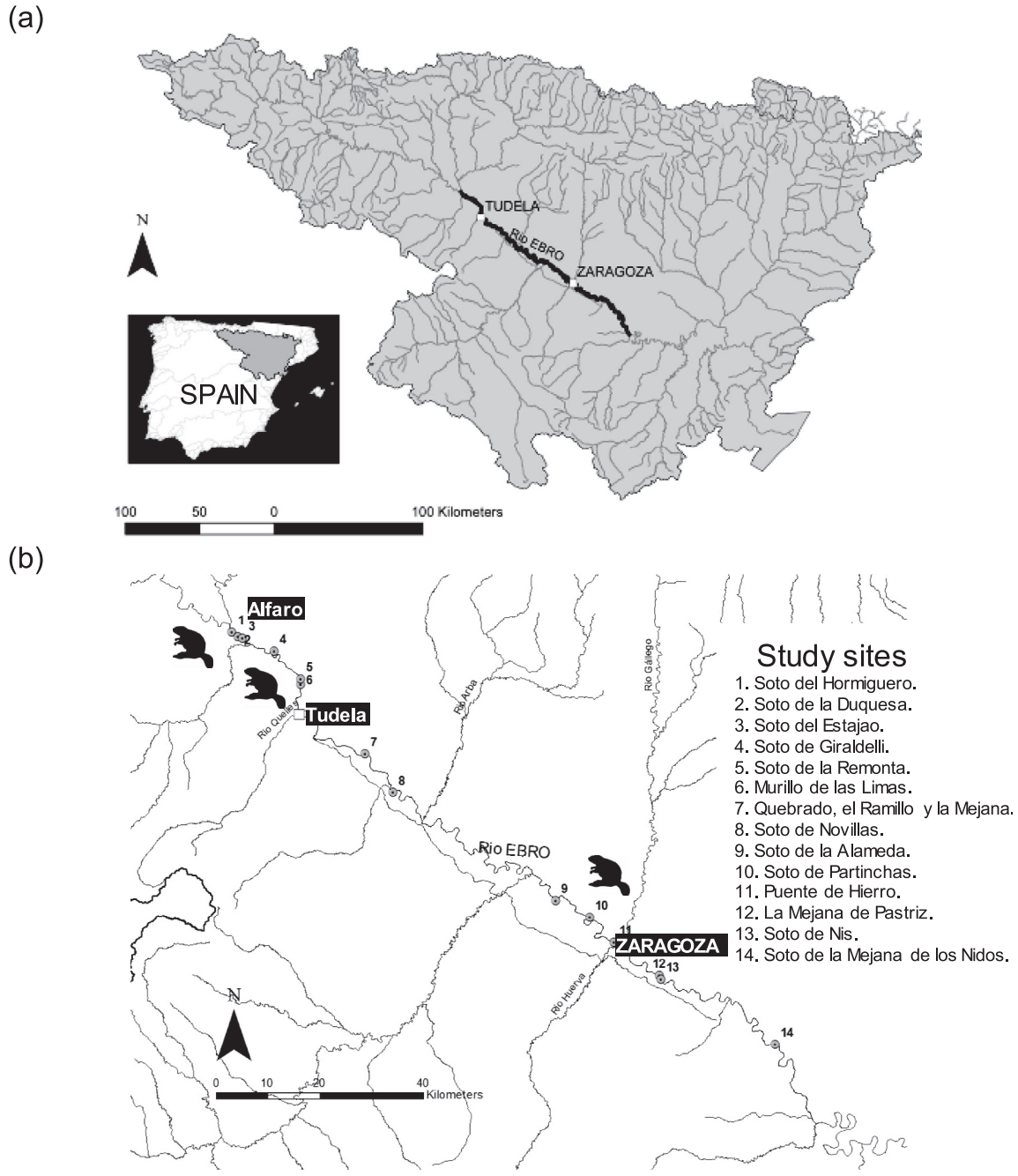

Fig. 1. (a) Study area located in the middle Ebro basin, north-eastern Spain showing the basin (grey area) and the location of main towns or cities (Tudela, Zaragoza). (b) Location of the 14 sampled riparian forests. The beaver (*Castor fiber*) silhouettes indicate the presence of this mammal species in forests located near Alfaro (Soto del Hormiguero), Tudela (Soto de La Remonta) and Zaragoza (Soto de Partinchas).

Dutch elm disease. Vines are also observed but with cover values below 5 % (*Hedera helix* L., *Vitis vinifera* L., *Humulus lupulus* L.). In some sites (e.g., Soto de Partinchas), scattered individuals of invasive or naturalized species such as *Laurus nobilis* L. are found. Lastly, we detected scars in tree stems of some riparian forests caused by the Eurasian beaver (*Castor fiber* L.) foraging activity (Table 1). This species was re-introduced in the study region in the 1990s.

2.2. Field sampling and data collection: stand composition, soils and deadwood

We selected 14 riparian forests based on their different conservation and maturity status in the middle Ebro basin (Table 1). In each site, we selected well-preserved stands and located from one to three 50-m long transects per site depending on the size of the forest (Table 2). We recorded the positions and elevations of the start and end of each transect using a GPS antenna attached to a tablet (resolution ±5 m). Transects were oriented perpendicular to the flow direction crossing different communities along the topographic gradient. Then, the distance and diameters at breast height (D.B.H.) and the tree height of the four closest neighbouring trees located in four different quadrants were measured every 2 m along the transect, annotating also the species identity and vigor (dead or living tree). Tree vigor was carefully considered in elms (*U. minor*), since individuals of these species with larger D.B.H. were often affected by Dutch elm disease.

In total, 19 transects were measured with 104 quadrants per transect. Using these data, we recorded the basal area and the density of each tree species using the point-quarter method (Cottam and Curtis, 1956). The importance value of each tree species in each site was obtained as the average of the relative density and basal area values of each tree species within each

Table 1
Names and composition of the fourteen riparian forests sampled along the middle Ebro basin. The sites number is indicated in Fig. 1b.

Number	Site	Town or city (region)	River side	No. transects	Beaver presence	Main tree species
1	Soto del Hormiguero	Alfaro (La Rioja)	Right	1	Yes	*Salix alba*, *Populus nigra*
2	Soto de la Duquesa	Alfaro (La Rioja)	Left	2	–	*Populus alba*, *Populus nigra*, *Fraxinus angustifolia*, *Ulmus minor*
3	Soto del Estajao	Alfaro (La Rioja)	Right	1	–	*Populus alba*, *Populus nigra*
4	Soto de Giraldelli	Castejón (Navarra)	Right	1	–	*Populus alba*, *Populus nigra*, *Salix alba*, *Fraxinus angustifolia*
5	Soto de la Remonta	Tudela (Navarra)	Right	3	Yes	*Populus alba*, *Populus nigra*, *Salix alba*, *Fraxinus angustifolia*, *Ulmus minor*
6	Murillo de las Limas	Tudela (Navarra)	Left	1	–	*Populus alba*,*Fraxinus angustifolia*, *Ulmus minor*
7	Quebrado, El Ramillo y la Mejana	Buñuel (Navarra)	Left	1	–	*Populus alba*, *Fraxinus angustifolia*, *Salix alba*, *Tamarix* spp.
8	Soto de Novillas	Novillas (Aragón)	Right	1	–	*Fraxinus angustifolia*, *Ulmus minor*, *Tamarix* spp.
9	Soto de la Alameda	Utebo (Aragón)	Right	1	–	*Salix alba*, *Fraxinus angustifolia*, *Ulmus minor*
10	Soto de Partinchas	Juslibol (Aragón)	Left	3	Yes	*Populus alba*, *Populus nigra*, *Fraxinus angustifolia*, *Salix alba*, *Ulmus minor*, *Tamarix* spp.
11	Puente de Hierro	Zaragoza (Aragón)	Right	–	–	*Ulmus minor*, *Populus alba*
12	La Mejana de Pastriz	Pastriz (Aragón)	Left	2	–	*Populus alba*, *Populus nigra*, *Salix alba*, *Ulmus minor*, *Tamarix* spp., *Acer negundo*
13	Soto de Nís	La Cartuja (Aragón)	Right	1	–	*Fraxinus angustifolia*, *Tamarix* spp.
14	Soto de la Mejana de los Nidos	Pina de Ebro (Aragón)	Right	1	–	*Salix alba*, *Tamarix* spp., *Populus nigra*, *Ulmus minor*

of the measured transects (Muller-Dombois and Ellenberg, 1974). Note that structure and deadwood data from forests located near Alfaro town (Soto del Hormiguero, Soto de la Duquesa, Soto del Estajao; Table 1) were already published by Camarero et al. (2023).

To characterize soil characteristics, we took soil samples at depths from 10 to 120 cm in five mature study forests (Table S1). Soils were basic (mean pH was 8.35) of the sandy, sandy-loamy, silt-loam and loamy types. The mean C and N soil concentrations were 6.61 % and 0.24 %, respectively, with a mean C/N ratio of 34.5. The soils are slightly saline with a mean conductivity of 1.63 dS m^{-1}.

To estimate the volume of lying deadwood we used an intercept method along vegetation transects (Van Wagner, 1968; Maser et al., 1988). We noted the cut-off points of intersection and the length of any pieces of dead wood >15 cm that intersected the vertical projection of the 50-m transects. Deadwood pieces were classified according to their decay degree considering five classes (cf. De Long et al., 2008): 1, intact wood, bark and branches; 2, incipient decay with intact bark but twigs (diameter < 3 cm) absent; 3, moderate decay, few remains of bark, no twigs, sapwood starts to decompose; 4, advanced decay, no bark or twigs and sapwood appears broken in small pieces; and 5, very decayed wood with only intact pieces of heartwood (see Fig. S7). We did not measure the basal area of stumps and snags.

2.3. Historical changes in river sinuosity

To characterize changes in sinuosity we analysed aerial photographs taken in the 14 study sites in four periods (1927, 1956, 1998–2003 and 2014–2015; see Figs. S8 and S9). We calculated the hydraulic sinuosity index (Mueller, 1968), i.e. the ratio between the curvilinear and the Euclidean distances between the end points of the channel, to summarize these dynamics. This was done by analysing aerial images with ArcGis ver. 10.0 (ESRI, Redlands, USA). We considered 2000-, 4000- and 6000-m long river segments measured upstream of each study site. We used in the final analyses data from the 4000-m segments given their higher stability compared with other resolutions. The river channel was digitized at scale 1:10000 following the axis of the main river wet channel over digitized aerial photos (1927) and over digital ortho-photographs for the other three periods.

We used the following cartographical sources for the four study periods: (i) 1927, 46 black and white digitized aerial photos (available at http://iber.chebro.es/geoportal/) which were geo-referenced in ArcGis 10.0 and the reference system used was ETRS-1989-UTM Zone; (ii) 1956–1957, black and white ortophotographs (available at Instituto Geográfico Nacional webpage http://www.ign.es/wms/pnoa-historico) for all sites excepting sites 8 and 14 which were not covered by this flight; (iii) 1998–2003, Spanish Ortophotographic Map or SIGPAC-FEGA flight at scale 1:40.000 (available at http://www.ign.es/wms/pnoa-historico) with sites 8, 9, 14 and 1–7 and 10–13 corresponding to the following flight years 1998, 1999, 2000 and 2003, in that order; and (iv) 2014–2015, with sites 1–7 and 8–14 corresponding to flight years 2014 and 2015, respectively (images available at http://idena.navarra.es and http://idearagon.aragon.es). In the analyses of 1927 images, the nearest neighbour resampling method was applied, and control points were chosen to avoid a concentration of points in specific regions of the images. Reference points were easily identifiable features and were not subject to significant spatio-temporal variations. The total error analysis parameter generated during the geographical referencing of the photographs was below 5 m in most cases.

2.4. Tree-ring width data

We selected two well-structured, mature riparian forests showing different historical river dynamics and located near Tudela (Soto de la Remonta) and Zaragoza (Soto de Partinchas). Their growth patterns were quantified and related to river flow. We sampled mature and dominant or co-dominant individuals of the main five tree species forming annual rings (*P. alba*, *P. nigra*, *F. angustifolia*, *U. minor* and *S. alba*). For each tree, two radial cores were taken at 1.3 m using 5 mm diameter Pressler borers (Haglöf, Sweden). Cores were dried at room temperature, glued on grooved wooden guides and sanded until the ring boundaries were distinguished. These samples were visually cross-dated (Fritts, 1976) and ring widths were measured with 0.01 mm resolution using a Lintab-TSAP semi-automatic device. Visual dating was verified using the COFECHA program which calculates correlations between the individual series and the average series of each species in each site (Holmes, 1983). Once the rings were measured and their dating verified, their widths were converted into basal area increment (BAI) assuming that the rings were concentric and considering only cores with pith or with inner rings located close to the pith.

The BAI series were detrended and standardized to eliminate the influence of changes in tree size and age or disturbances using 30-year long cubic smoothing splines (Klesse, 2021). Then, bi-weight robust averages were calculated to obtain mean series of BAI residuals. This allowed having well-replicated BAI series of the five species in the two sites for the common period 1990–2016 (Table S2), when most series (excepting *P. nigra* from Zaragoza and *S. alba* from both sites) showed values of the Expressed Population Signal higher than 0.85 (Wigley et al., 1984). These procedures were done using the dplR package (Bunn, 2010; Bunn et al., 2022).

To illustrate tree growth changes in urban sites located in the Zaragoza city we also sampled: (i) *P. alba* trees in a forest located downstream (La Mejana de Pastriz), and (ii) living (n = 20 individuals) and dead *U. minor* trees (n = 20 individuals) coexisting in an urban area near the river (Puente de Hierro). These were natural stands selected to investigate whether: (i) the building of a weir between 2007 and 2008 during the Expo-2008 international exposition in Zaragoza affected *P. alba* growth downstream, and (ii) dead elms showed lower growth in response to the severe 2012 drought which also reduced the winter river flow (Rodríguez-González et al., 2021).

Table 2
Main structural variables (stem density, basal area and importance value) calculated for the main tree and vine species or riparian forests sampled along the middle Ebro basin. In some sites several transects were measured. Density and basal area are separately presented for living and dead trees. Species' abbreviations: Pa, *Populus alba*; Pn, *Populus nigra*; Sa, *Salix alba*; Fa, *Fraxinus angustifolia*; Um, *Ulmus minor*; Ta, *Tamarix* spp.; Cm, *Crataegus monogyna*; An, *Acer negundo*; Ma, *Morus alba*; Pc, *Prunus cerasus*; Ln, *Laurus nobilis*; Vv, *Vitis vinifera*.

Site	No. transect	Tree species	Stem density living / dead (ind ha^{-1})	Basal area living / dead (m^2 ha^{-1})	Importance value
Soto del Hormiguero	1	Sa	300	20.63	0.35
		Pn	1250	19.77	0.65
Soto de la Duquesa	1	Cm	50	0.12	0.01
		Vv	100	0.08	0.03
		Ta	50	0.14	0.01
		Fa	200	5.76	0.09
		Pn	500	28.61	0.28
		Pa	550	59.02	0.44
		Um	300 / 250	9.18 / 11.86	0.13
	2	Cm	100	0.27	0.04
		Ln	100	3.15	0.05
		Pn	200	99.93	0.47
		Um	450 / 100	3.43 / 1.71	0.20
		Fa	350	21.94	0.23
Soto del Estajao	1	Um	50	0.06	0.02
		Fa	50	0.10	0.02
		Pa	150	24.54	0.18
		Pn	300	45.86	0.34
		Sa	500	46.60	0.44
Soto de Giraldelli	1	Fa	100	0.02	0.06
		Pn	450	60.46	0.66
		Sa	350	13.92	0.29
Soto de la Remonta, wide part	1	Sa	50	0.17	0.03
		Fa	100	1.26	0.07
		Pn	650 / 50	53.16 / 1.13	0.89
	2	Fa	150	10.15	0.16
		Pa	250	38.23	0.47
		Um	650 / 300	6.41 / 3.09	0.37
Soto de la Remonta, narrow part	1	Cm	50	0.08	0.03
		Fa	100	11.55	0.16
		Pa	150	40.88	0.44
		Um	550 / 100	6.01 / 2.92	0.37
Murillo de las Limas	1	Pa	150	19.80	0.30
		Ta	100	2.16	0.07
		Fa	50	8.13	0.12
		Um	750 / 250	13.25 / 5.29	0.51
Quebrado, El Ramillo y la Mejana	1	Sa	50	11.88	0.14
		Ta	500	4.17	0.28
		Fa	350	20.09	0.37
		Pa	150	12.98	0.20
Soto de Novillas	1	Cm	50	0.19	0.01
		Pc	300	0.97	0.08
		Ta	250	3.54	0.09
		Fa	600	16.42	0.29
		Pa	450	36.42	0.42
		Um	350	1.28	0.10
Soto de la Alameda	1	Ta	1250	16.46	0.57
		Sa	250	37.15	0.43
Soto de Partinchas	1	Ta	800	4.13	0.17
		Sa	2000 / 50	41.04 / 1.01	0.76
		Pn	300	1.50	0.06
	2	Cm	50	0.12	0.02
		Pn	50	13.21	0.12
		Um	850 / 250	4.15 / 2.56	0.35
		Fa	200	6.79	0.13
		Pa	200 / 50	40.24 / 9.43	0.39
	3	Cm	50	0.15	0.02
		Fa	250	13.84	0.18
		Pa	450	55.89	0.52
		Um	600 / 100	8.39 / 2.95	0.28
La Mejana de Pastriz	1	An	100	1.66	0.07
		Ta	50	1.99	0.04
		Sa	0 / 50	0.00 / 0.28	0.00
		Fa	50	4.65	0.06
		Pn	50 / 50	6.13 / 17.37	0.07
		Um	0 / 50	0.00 / 0.77	0.00
		Pa	550 / 50	59.54 / 0.48	0.75
	2	Um	150 / 50	1.12 / 1.76	0.10
		Ta	0 / 50	0.00 / 1.01	0.00
		Fa	100	1.06	0.07
		Pa	600	55.61	0.83

(continued on next page)

Table 2 (*continued*)

Site	No. transect	Tree species	Stem density living / dead (ind ha^{-1})	Basal area living / dead (m^2 ha^{-1})	Importance value
Soto de Nís	1	Fa	650	17.99	0.75
		Ta	300	4.17	0.25
Soto de la Mejana de los Nidos	1	Ta	500	4.24	0.36
		Ma	100	0.19	0.06
		Pn	100	1.45	0.08
		Um	50	0.25	0.03
		Sa	100	25.90	0.46

The BAI residual series were correlated with seasonal river flow data since previous studies showed that Mediterranean riparian forests respond to changes in river flow (Camarero et al., 2021, 2023; Rodríguez-González et al., 2014, 2021).

2.5. Statistical analyses

Normality of data and variance homogeneity were tested using Kolmogorov-Smirnov and Barlett tests, respectively. The Kendall τ test was used to quantify the trends of annual climate variables. A generalized linear model (logistic model) was fitted to *U. minor* trees sampled in all sites as a function of D.B.H. to predict their mortality probability (n = 180 individuals). These trees were classified as living or dead (fully defoliated, dead shoots and branches, stem with broken and falling bark and abundant galleries made by beetle barks) individuals, respectively. The model was based on a binomial distribution and it was fitted by using maximum likelihood estimation with the R glm function (Venables and Ripley, 2002).

We used a Non-Metric Multidimensional Scaling (NMDS) ordination to summarize the information on: historical changes in river sinuosity, forest composition (importance values) and amount and decay degree of deadwood (Legendre and Legendre, 2012). The river sinuosity values in different periods (1927, 1956, 1998–2003 and 2014–2015) were entered into the analyses as environmental variables, whilst response variables were the importance values of the main tree species, deadwood volume and the relative amounts of deadwood grouped according to decay degree. To assess relationships between variables, Spearman correlations (r_s) were calculated among the variables considered in the NMDS including also the mean, standard deviation (SD) and coefficient of variation (CV) of the sinuosity index values (Table S3). The NMDS was calculated using the vegan package (Oksanen et al., 2022). All analyses were carried out in R (R Development Core Team, 2022).

3. Results

3.1. Historical river dynamics according to changes in the sinuosity index

Most study sites have lost sinuosity or kept stable sinuosity indices from 1927 to 2015 (ratios between sinuosity values of both dates ≤1). In 1927, the mean ± SD river sinuosity index was 1.39 ± 0.36, in 1956 it was 1.30 ± 0.31, and then it declined to 1.20 ± 0.12 in 1998–2015. The 1927 sinuosity was significantly larger than the 2015 sinuosity (t = 2.03, p = 0.04). The sinuosity indices of periods 1998–2003 and 2014–2015 were significantly correlated (r = 0.98, p < 0.001).

The site sinuosity CV considering the four study periods was 13.3 % with maximum values in some places such as Soto de Nis (42.9 %) or Soto de la Duquesa (28.7). The CV values were low in other sites located near Tudela town, such as Soto de Quebrado, El Ramillo y la Mejana (0.9 %) and Soto de la Remonta (3.1 %), and near Zaragoza city (e.g., Puente de Hierro, 0.9 %) (Fig. 2).

The two intensively studied riparian forests presented different historical river dynamics with a higher recent sinuosity in Soto de Partinchas (1.16) and Soto de la Remonta (1.06), but with a higher historical loss of sinuosity in the first (ratio of 2005/1927 sinuosity values, 0.66) than in the second site (ratio of 2005/1927 sinuosity values, 0.89).

3.2. Historical changes in river sinuosity, stand structure and deadwood volume

Sites with high sinuosity values in 1956 (significantly higher than the 1956 mean, t = 2.23, p < 0.05) corresponded to mature stands with large trees and abundant deadwood with moderate to advanced decay (Tables 2 and 3).

In forests sampled near Tudela and Zaragoza, the trees with thickest stems corresponded to *P. nigra* and *F. angustifolia*, followed by *P. alba* (Fig. 3). This led to higher basal area and deadwood volume values in Tudela forests (Tables 2 and 3). So, the mean deadwood volume was 145 ± 91 m^3 ha^{-1}, with maximum and minimum values recorded in Soto de la Remonta (350 m^3 ha^{-1}) and Soto de Partinchas (20 m^3 ha^{-1}), respectively (Table 3). In these two sites D.B.H. and tree height of the main tree species were positively and significantly (p < 0.05) correlated (Fig. S10), as well as D.B.H. and the bark thickness (Fig. S11). In general, the site deadwood volume and the total basal area were not related (r_s = −0.11, p = 0.65). Moreover, the death probability of *U. minor* trees was above 50 % for individuals with D.B.H. > 23.5 cm (Fig. S12).

The NDMS plot grouped sites with high sinuosity values in 1927 and also with a high sinuosity CV due to long-term declines (e.g., Soto de Nis) or increases (e.g., Soto del Hormiguero) in river sinuosity (Table 1, Fig. 4). In contrast, other sites have showed low sinuosity values during the whole study period and, therefore, presented low CV values (e.g., Puente de Hierro, Mejana de los Nidos). Other sites show high CV values, but relatively high sinuosity values (e.g., Soto de la Duquesa).

Sinuosity indices measured from 1998 to 2015 were negatively related to the importance values of *F. angustifolia* (r_s = −0.83, p < 0.001) and *P. alba* (r_s = −0.64, p = 0.02) (Table S3). The importance value of *P. alba* was positively related to the importance value of *U. minor* and the relative abundance of moderately to very decayed deadwood. The importance value of *P. nigra* was negatively related to the importance value of *Tamarix* spp. Another negative relationship was found between *F. angustifolia* and *S. alba*, with the latter species being abundant in sites with abundant scarcely decayed deadwood.

3.3. Growth patterns and responses to river flow

In Soto de la Remonta, the BAI residuals of *F. angustifolia* and *P. nigra* were positively correlated in the common period 1990–2016 (r = 0.47, p = 0.01), whereas a similar positive association was found for *F. angustifolia* and *U. minor* in Soto de Partinchas (r = 0.47, p = 0.01) (Fig. 5). In Soto de la Remonta, the BAI residuals of *S. alba* and *P. nigra* were negatively related (r = −0.63, p = 0.003).

The BAI residuals responded more to changes in river flow in Soto de Partinchas than in Soto de la Remonta, particularly in the case of *F. angustifolia* (Table 4). Tree species mainly responded to changes in winter and spring river flow, excepting *P. nigra* which mainly responded to the previous autumn flow. A high summer river flow was positively related to high growth rates, mainly in *U. minor* and *S. alba*. The highest correlation (r = 0.66) was found between spring river flow and *U. minor* BAI residuals in Soto de Partinchas, a site where abundant dead *U. minor* trees were found (Fig. 3).

The correlation between growth series of *P. alba* individuals growing downstream Zaragoza increased after the weir building (Fig. 6a). Correlations (mean ± SD) were significantly (Mann-Whitney test, U = 78,

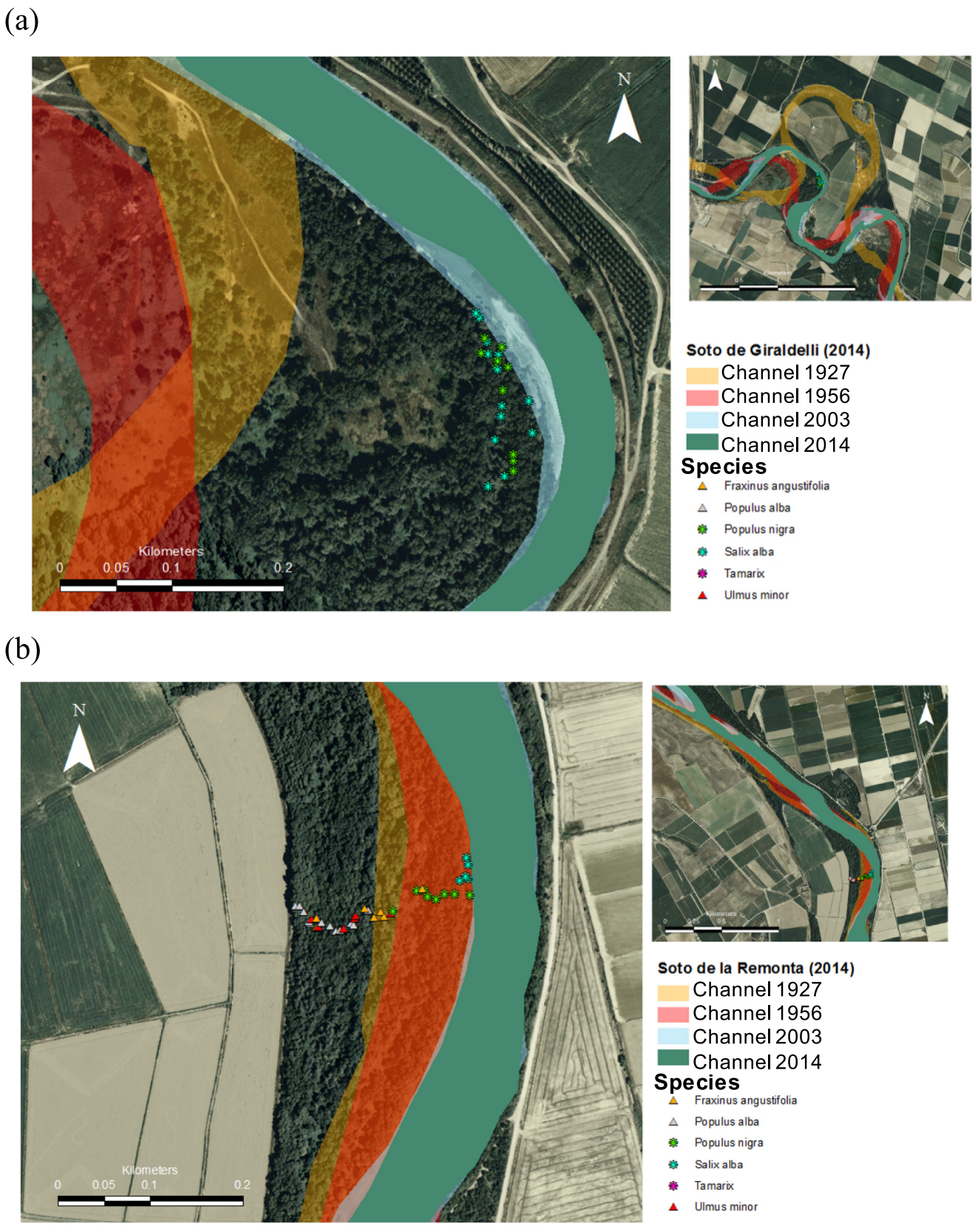

Fig. 2. Contrasting historical dynamics of the Ebro river sinuosity in two riparian forests sampled near Tudela, north-eastern Spain. Changes in the river channel from 1927 (yellow area) to 1956 (red area), 2003 (light blue area) and 2014 (green area) in the (a) Soto de Girardelli and (b) Soto de la Remonta. Symbols show the sampled trees. The inset shows the changes in channel at a large scale.

Table 3
Data of deadwood volume and decay class (from I –low– to V –high– decay degree) in the study riparian forests.

Site	Transect number	Deadwood volume (m^3 ha^{-1})	Deadwood volume according to decay class (%)				
			1	2	3	4	5
Soto del Hormiguero	1	260	0.77	85.36	13.87	0.00	0.00
Soto de la Duquesa	1	100	0.00	14.32	35.82	49.86	0.00
		200	0.00	0.00	16.20	83.80	0.00
	2						
Soto del Estajao	1	40	0.00	2.82	78.87	18.31	0.00
Soto de Giraldelli	1	220	0.00	81.26	17.61	1.12	0.00
Murillo de las Limas	1	250	0.00	13.30	86.70	0.00	0.00
Soto de la Remonta, wide part	1	350	0.29	3.64	94.26	1.81	0.00
		260	1.95	86.02	12.03	0.00	0.00
	2						
Soto de la Remonta, narrow part	1	160	0.00	60.85	13.91	25.24	0.00
Quebrado. El Ramillo y la Mejana	1	60	0.00	95.24	4.76	0.00	0.00
Soto de Novillas	1	160	0.00	15.62	78.13	6.25	0.00
Soto de la Alameda	1	170	0.00	2.88	25.18	71.94	0.00
Soto de Partinchas	1	20	0.42	46.77	37.57	15.24	0.00
		70	0.00	27.71	64.52	6.89	0.00
	2						
		90	0.00	0.00	54.29	35.28	5.07
	3						
La Mejana de Pastriz	1	60	0.00	67.39	31.52	1.09	0.00
		110	0.00	0.00	86.95	7.68	5.37
	2						
Soto de Nís	1	60	0.00	100.00	0.00	0.00	0.00
Soto de la Mejana de los Nidos	1	110	100.00	0.00	0.00	0.00	0.00

$p < 0.001$) higher after 2007 (0.86 ± 0.11) than before (0.23 ± 0.52). In addition, recently dead *U. minor* trees growing in the Zaragoza city river banks showed a significantly (Mann-Whitney test, $U = 4, p < 0.01$) smaller growth rates after the 2012 drought (1.8 ± 0.9 mm) than surviving (4.6 ± 1.1 mm) *U. minor* individuals (Figs. 6b). Growth rates of *U. minor* trees in this site were also lower than those observed in a nearby forest (Soto de Partinchas), which showed a better recovery after the 2011–2012 drought (Fig. S13).

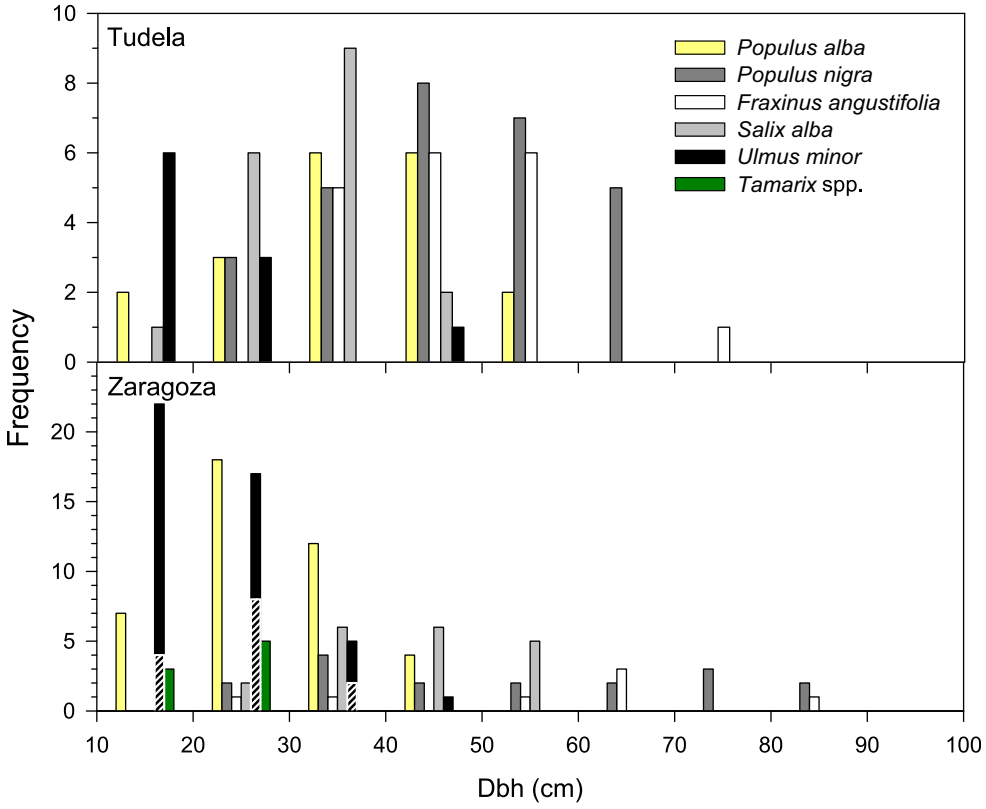

Fig. 3. Size structures (Dbh, diameter at breast height) of the main tree species sampled in riparian forests located near Tudela (Soto de Giraldelli, Soto de la Remonta, Murillo de las Limas, Soto de Quebrado, El Ramillo y la Mejana) and Zaragoza (Soto de Novillas, Soto de la Alameda, Soto de Partinchas, La Mejana de Pastriz) sites. In the bars corresponding to elms (*Ulmus minor*) the hatched area indicates dead individuals.

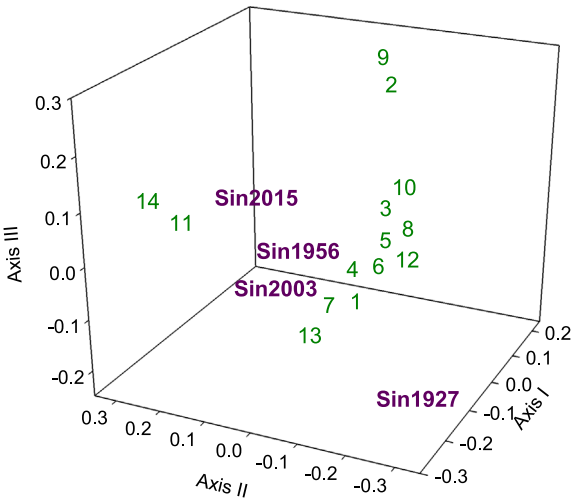

Fig. 4. NMDS plot showing the scores in three axes of the 14 riparian forests (green symbols; see numbers in Table 1) and the river sinuosity (purple symbols) in 1927, 1956, 2003 and 2015.

4. Discussion

The channel sinuosity decreased from 1927 to 2015 in response to the historical regulation of the Ebro river. Currently, riparian forests with low sinuosity indices, i.e. characterized by a linear stream geomorphology, are dominated by less (e.g., *F. angustifolia*) and more phreatophytic species (e.g., *P. nigra*), partially supporting our hypotheses. This pattern may be explained because the distribution of tree species along the riverbank topographic gradient has historically narrowed reflecting a mixture of more phreatophytic species, usually found near the river (e.g., *S. alba*, *Tamarix* spp.), and less phreatophytic species (e.g., *F. angustifolia*, *U. minor*). The historical loss of channel sinuosity and the contraction of riparian forests are related to anthropic impacts leading to a disconnection of active channel from floodplain. Historical channel migration may put trees in different habitat types in relation to the habitat where they regenerated and established, promoting the mixing of tree species with different water uptake strategies. This would explain the co-occurrence of *P. alba* and *U. minor* and their dominance in sites with abundant moderately to very decayed deadwood where river flow is slow. In contrast, pioneer and more phreatophytic tree species such as *S. alba* were associated to sites with scarcely decayed deadwood where river flow or frequent floods transport large wood pieces (Le Lay et al., 2013). In addition, the intensive agricultural uses of water for irrigation near several study forests (e.g., Soto de la

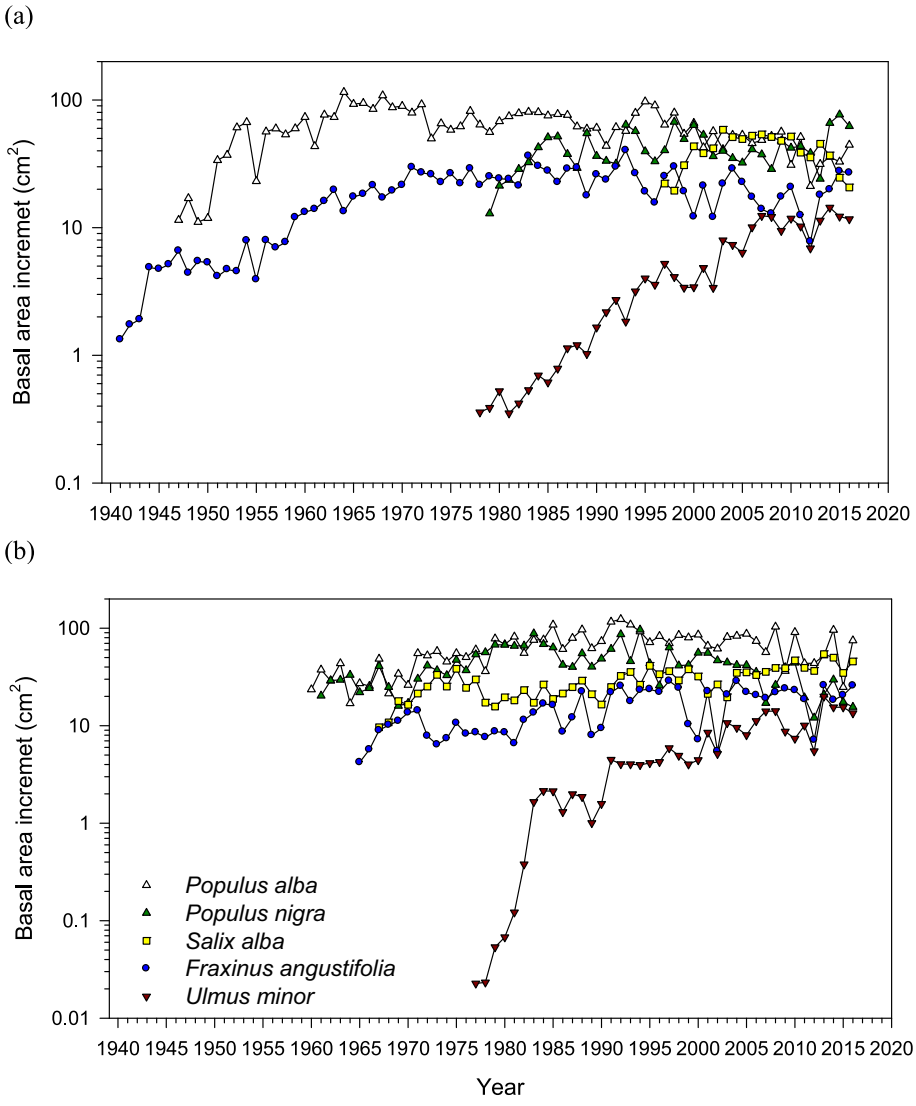

Fig. 5. Growth data (basal area increment, log scale) of the main tree species sampled in (a) Tudela (Soto de la Remonta) and (b) Zaragoza (Soto de Partinchas) riparian forests.

Table 4
Pearson correlations calculated between basal-area increment residuals of five tree species sampled in two study forests and seasonal river flow data. Months abbreviated by lowercase letters correspond to the prior year, whereas months abbreviated by uppercase letters correspond to the growth year. Bold values are significant correlation coefficients ($p < 0.05$).

Site	Species																			
	P. alba				*P. nigra*				*F. angustifolia*				*S. alba*				*U. minor*			
	son	dJF	MAM	JJA	son	dJF	MAM	JJA	son	dJF	MAM	JJA	son	dJF	MAM	JJA	son	dJF	MAM	JJA
Soto de la Remonta	0.17	0.07	0.19	0.20	**0.43**	0.17	0.14	0.32	0.28	**0.43**	0.26	0.07	0.15	0.07	0.20	0.31	−0.05	0.13	**0.39**	0.35
Soto de Partinchas	0.20	0.21	0.20	**0.38**	0.29	0.26	0.06	0.11	0.17	**0.51**	**0.39**	0.34	0.26	0.06	0.03	**0.46**	0.02	0.32	**0.66**	**0.57**

Duquesa, Soto de la Remonta, Soto de Partinchas) or the aridification trend observed in the study area, could also have affected the groundwater use of the study species. Future studies could address this issue by analysing isotopic composition (δ^2H, $\delta^{18}O$) in water, soil and xylem samples and relate them to changes in river flow and water table depth (Singer et al., 2013). Overall, river regulation and the reduction of regular floods in large rivers could lead to an over-mature state of some forests benefiting less phreatophytic, terrestrial tree species (Janssen et al., 2020; Havrdová et al., 2023) such as *F. angustifolia* (Janík et al., 2016; Camarero et al., 2021; Rodríguez-González et al., 2021).

Our hypotheses on river-growth couplings were supported since river flow diversion after the weir building in Zaragoza led to growth reduction and increased growth coherence among *P. alba* trees downstream. Similar results were observed by Stella et al. (2013) and Schook et al. (2020)

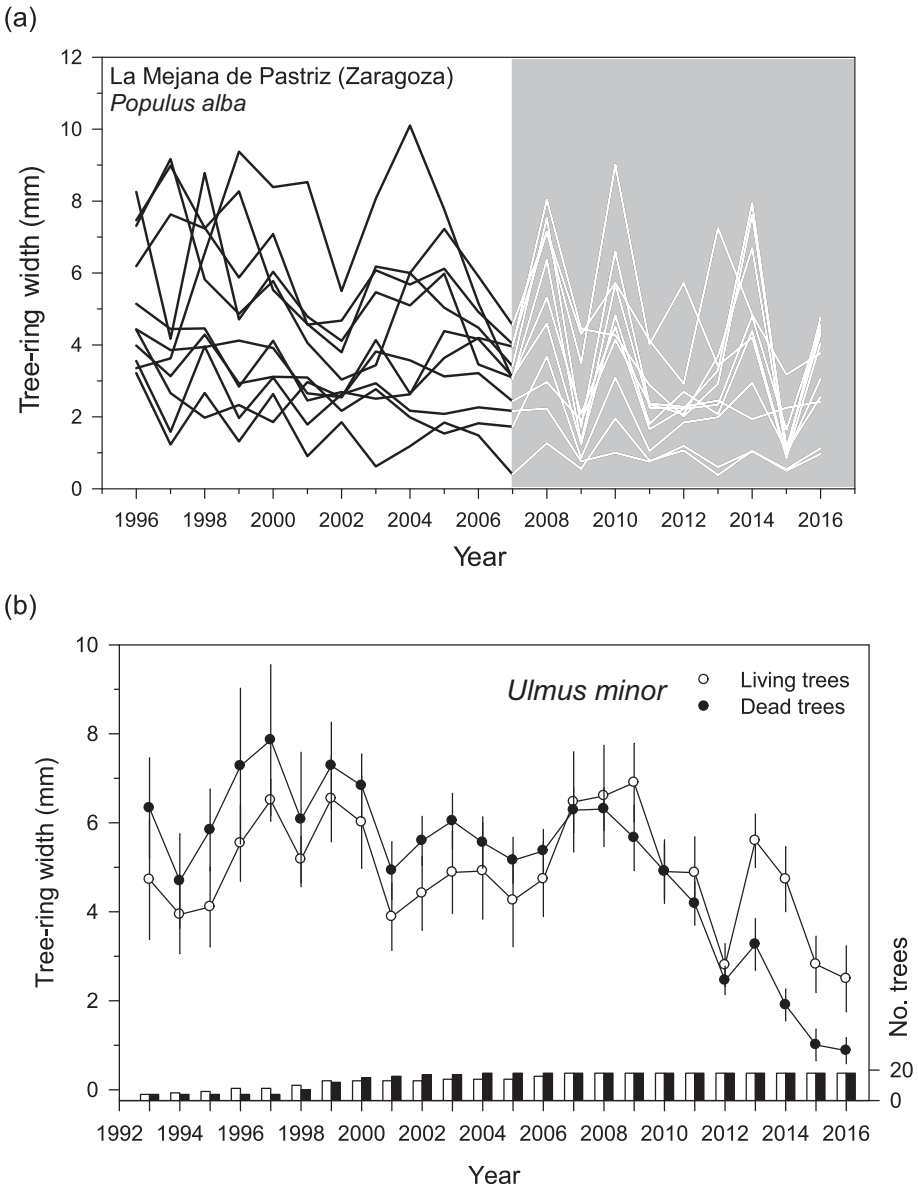

Fig. 6. Changes in tree growth illustrating recent modifications in land use along the middle Ebro basin. (a) Growth decline and became more coupled between trees (grey area) in the case of *P alba* (La Mejana de Pastriz site, located Zaragoza downstream) after a weir was built upstream in 2007–2008. (b) Dead elm (*U. minor*) trees (black symbols and bars) located in the Zaragoza city river banks showed lower growth in response to the severe 2012 drought than surviving trees (white symbols and bars). The elms trees were sampled near Puente de Hierro site in Zaragoza city. Values are means ± SD and the bars show the annual number of sampled trees (right y axis).

who found that geomorphic alteration (gravel mining) or flow diversion reduced carbon assimilation, basal growth rate and tree survival triggering canopy dieback and death of riparian forests. Flow diversion after dam building also reduced soil moisture, stand leaf area and root biomass (Williams and Cooper, 2005). Phreatophytic riparian cottonwoods are prone to drought stress, which leads to branch and shoot death due to xylem cavitation (Tyree et al., 1994; Phelan et al., 2022). In these *Populus* species, the observed growth decline could precede crown dieback and increased mortality due to altered river geomorphology. Therefore, interactions between hydrogeomorphic changes and river flow may predispose to canopy dieback and death of riparian tree species (Williams and Cooper, 2005; Stella et al., 2013; Rood and Mahoney, 2023).

Drought and the loss of river sinuosity jointly contributed to *U. minor* growth decline in the urban site (Puente de Hierro), in agreement with the pronounced sensitivity of this species to changes in spring river flow documented here. This species shows strong and negative impacts of water shortage on radial growth, particularly in provenances susceptible to Dutch elm disease (Pita et al., 2018). This means that hydrological and climatic droughts lead to long-term growth decline and dieback of sampled elm trees, increasing their vulnerability to low spring river flow (Tulik et al., 2020; Valor et al., 2020; Kibler et al., 2021), even if the ultimate causes of tree mortality are pathogens (e.g., Colangelo et al., 2018; Martín et al., 2019).

The deadwood amount and its decay degree are important proxies of biodiversity for belowground fungal diversity (Birch et al., 2023). In the study area, the co-occurrence of *P. alba* and *U. minor* and its presence in sites with moderately to highly decayed deadwood may be the result of the contraction of riparian forests and the disconnection of active channel vs. floodplain leading to the accumulation of old deadwood, which can result in an increased local abundance of fungi and wood-boring insects. Such mixing of species with contrasting water use strategies and slowed river dynamics may explain why deadwood volume did not increase as stand basal area did, in contrast with what Oettel et al. (2022) found in the Danube river basin.

In agreement with previous studies (e.g., Cabezas et al., 2009), we found that the historical Ebro river dynamics and forest composition were altered by historical flow regulation. The decrease in river sinuosity may be linked to less diverse riverscapes where mature *F. angustifolia* stands dominate, as we found, and extremes pulses of river discharge are lower nowadays than in 1927 due to river regulation. In riparian forests from eastern France, changes in channel elevation also affected common ash (*Fraxinus excelsior*) growth and recruitment (Dufour and Piégay, 2008).

The losses of ecosystem services provided by riparian forests due to deficient instream flow regimes, drought and geomorphic alterations are extensive and long-lasting (Andersen, 2016). Therefore, proactive strategies such as keeping environmental flows with a functional flow approach would help to protect and restore a broad suite of ecological, geomorphic and biogeochemical functions (Stein et al., 2021). These strategies would be more efficient during spring and in seasonally dry regions such as the study area to alleviate drought stress and avoid the mismatch of the flow regime relative to the functioning of riparian tree species (Yarnell et al., 2015). Restoration programs of the Ebro river-forest system could use some of the 1927 conditions as a reference or guiding situation, reallocate or remove some structures (dykes, weirs) to restore flow regime and lower floodplain heights. However, current hydrologic, socio-economic and landscape constraints at basin to reach scales must be also considered (Dufour and Piégay, 2009). For instance, stakeholders must be involved in the restoration process to decide which sites are more appropriate for poplar or ash conservation. Restoration strategies should also consider climate extremes such as droughts and lasting reductions of river flow (e.g., Camarero, 2022; Schook et al., 2022).

5. Conclusions

Sinuosity in the middle Ebro Basin decreased leading to accumulation of less-decayed deadwood and favouring non-phreatophytic tree species such as *F. angustifolia* as hypothesized. Sites with high sinuosity values in 1956 corresponded to mature stands dominated by *P. nigra*. Sinuosity in recent periods was negatively related to *F. angustifolia* and *P. alba* abundance, whereas sites where *P. alba* and *U. minor* co-occurred were characterized by moderately to very decayed deadwood. These patterns are caused by a loss of river sinuosity and a contraction of the riverbank gradient increasing disconnection of active channel from floodplain, with a mixing of more (e.g., *P. nigra*) and less phreatophytic species (e.g., *U. minor*). River flow diversion reduced growth and increased the tree-to-tree *P. alba* growth coherence making the affected stands prone to drought-induced dieback. Hydrological droughts also contributed to growth decline of *U. minor*, which is very sensitive to changes in spring river flow.

Our findings show that riparian forests react to the interaction of multiple stressors including: (i) historical anthropic modifications of the natural flow regime and geomorphology, such as lower river flow and the disconnection of the active channel vs floodplain, which often results in lower flow in relation to riparian species, and (ii) climatic and hydrological droughts. Historical alteration of river regimes can enhance less phreatophytic tree species. These changes can be the result of water diversion effect through the reduction in river flow, but also due to the inversion of the natural regime (e.g., excess of irrigation water being returned to the river in dry periods). Impacts of regional droughts and local river flow diversion on riparian forests are mediated by site-contingent conditions including historical geomorphic changes, topographic position, invasive pathogens, climate conditions and forest composition. Droughts are likely to compound the effects of reduced precipitation and low river flow, due to reduced rainfall, changes in spring snowmelt timing and increased demand for agricultural uses, thus resulting in reduced productivity and riparian forest dieback. Historical analyses should be used to design environmental flow regimes to reduce drought stress, growth decline and tree mortality.

CRediT authorship contribution statement

J. Julio Camarero: Conceptualization, Formal analysis, Funding acquisition, Investigation, Methodology, Writing – original draft, Writing – review & editing. **Michele Colangelo:** Data curation, Funding acquisition, Investigation, Methodology, Writing – review & editing. **Patricia M. Rodríguez-Gonzalez:** Formal analysis, Funding acquisition, Methodology, Writing – review & editing.

Data availability

Data will be made available on request.

Declaration of competing interest

Authors declare no conflict of interest.

Acknowledgments

We thank Ángela Sánchez-Miranda and Raúl Sánchez-Salguero for their help in the field. This study was supported by the BBVA Foundation (SEDIBER project). PMRG was supported by Portuguese Foundation for Science and Technology (FCT), through CEEC Individual program grant number 2020.03356.CEECIND, Forest Research Centre is a research unit funded by FCT (UIDB/00239/2020) and Associate Laboratory TERRA is funded by FCT (TERRA - LA/P/0092/2020). This study was also supported by STSM 40285 “Long-term growth and functioning of a major tree species in Mediterranean floodplain forests” to M. Colangelo, funded by COST Action (CA16208) – CONVERGES: Knowledge Conversion for Enhancing Management of European Riparian Ecosystems and Services.

Appendix A. Supplementary data

Supplementary data to this article can be found online at https://doi.org/10.1016/j.scitotenv.2023.165266.

References

Andersen, D., 2016. Climate, streamflow, and legacy effects on growth of riparian *Populus angustifolia* in the arid San Luis Valley, Colorado. J. Arid Environ. 134, 104–121.

Ayerra, E., 1988. Los sotos de la ribera Tudelana. Servicio de Medio Ambiente del Gobierno de Navarra, Pamplona, Spain.

Birch, J.D., Lutz, J.A., Struckman, S., Miesel, J.R., Karst, J., 2023. Large-diameter trees and deadwood correspond with belowground ectomycorrhizal fungal richness. Ecol. Process. 12, 3. https://doi.org/10.1186/s13717-022-00415-8.

Broadmeadow, S., Nisbet, T.R., 2004. The effects of riparian forest management on the freshwater environment: a literature review of best management practice. Hydrol. Earth Syst. Sci. 8, 286–305.

Bunn, A.G., 2010. Statistical and visual crossdating in R using the dplR library. Dendrochronologia 28, 251–258. https://doi.org/10.1016/j.dendro.2009.12.001.

Bunn, A., Korpela, M., Biondi, F., Campelo, F., Mérian, P., Qeadan, F., Zang, C., 2022. dplR: Dendrochronology Program Library in R. R Package Version 1.7.4. https://CRAN.R-project.org/package=dplR.

Cabezas, A., Comín, F.A., Beguería, S., Trabucchi, M., 2009. Hydrologic and landscape changes in the Middle Ebro River (NE Spain): implications for restoration and management. Hydrol. Earth Syst. Sci. 13, 273–284.

Camarero, J.J., 2022. ENSO signals recorded by ash tree rings in Iberian riparian forests. Water 14, 3027.

Camarero, J.J., Colangelo, M., Rodríguez-González, P.M., Sánchez-Miranda, A., Sánchez-Salguero, R., Campelo, F., Rita, A., Ripullone, F., 2021. Wood anatomy and tree growth covary in riparian ash forests along climatic and ecological gradients. Dendrochronologia 70, 125891.

Camarero, J.J., Colangelo, M., Rodríguez-González, P.M., 2023. Tree growth, wood anatomy and carbon and oxygen isotopes responses to drought in Mediterranean riparian forests. For. Ecol. Manag. 529, 120710.

Charles, F., Garrigue, J., Coston-Guarini, J., Guarini, J.-M., 2022. Estimating the integrated degradation rates of woody debris at the scale of a Mediterranean coastal catchment. Sci. Total Environ. 815, 152810. https://doi.org/10.1016/j.scitotenv.2021.152810.

Colangelo, M., Camarero, J.J., Ripullone, F., Gazol, A., Sánchez-Salguero, R., Oliva, J., Redondo, M.A., 2018. Drought decreases growth and increases mortality of coexisting native and introduced tree species in a temperate floodplain forest. Forests 9, 1–17.

Collins, B.D., Montgomery, D.R., Haas, A.D., 2002. Historical changes in the distribution and functions of large wood in Puget Lowland rivers. Can. J. Fish. Aquat. Sci. 59, 66–76.

Cortina-Segarra, J., García-Sánchez, I., Grace, M., Andrés, P., Baker, S., Bullock, C., Decleer, K., Dicks, L.V., Fisher, J.L., Frouz, J., Klimkowska, A., Kyriazopoulos, A.P., Moreno-Mateos, D., Rodríguez-González, P.M., Sarkki, S., Ventocilla, J.L., 2021. Barriers to ecological restoration in Europe: expert perspectives. Restor. Ecol. 29, e13346.

Cottam, G., Curtis, J.T., 1956. The use of distance measure in phytosociological sampling. Ecology 37, 451–460.

De Long, S.C., Sutherland, G.D., Daniels, L.D., Heemskerk, B.H., Storaunet, K.O., 2008. Temporal dynamics of snags and development of snag habitats in wet spruce-fir stands in east-central British Columbia. For. Ecol. Manag. 255, 3613–3620.

Dixon, S.J., Sear, D.A., Nislow, K.H., 2019. A conceptual model of riparian forest restoration for natural flood management. Water Environ. J. 33, 329–341.

Dufour, S., Piégay, H., 2008. Geomorphological controls of *Fraxinus excelsior* growth and regeneration in floodplain forests. Ecology 89, 205–215.

Dufour, S., Piégay, H., 2009. From the myth of a lost paradise to targeted river restoration: forget natural references and focus on human benefits. River Res. Appl. 25, 568–581.

Fernández-González, F., Molina, A., Loidi, J., 1990. Los tarayales de la depresión del Ebro. Acta Bot. Malac. 15, 311–322.

Ferreira, T., Globevnik, L., Schinegger, R., 2018. Water Stressors in Europe: New Threats in the Old World. Multiple Stressors in River Ecosystems. Chapter. 8. Elsevier, pp. 139–155.

Fritts, H.C., 1976. Tree Rings and Climate. Academic Press, London, UK.

Frutos, L.M., Ollero, A., Sánchez-Fabre, M., 2004. Caracterización del Ebro y su cuenca y variaciones en su comportamiento hidrológico. In: Gil Olcina, A. (Ed.), Alteración de los regímenes fluviales peninsulares. Fundación Cajamurcia, Murcia, Spain, pp. 233–280 (Coord.).

Gurnell, A.M., 2014. Plants as river system engineers. Earth Surf. Process. Landf. 39, 4–25.

Gurnell, A.M., Piegay, H., Swanson, F.J., Gregory, S.V., 2002. Large wood and fluvial processes. Freshw. Biol. 47, 601–619.

Gurnell, A.M., Scott, S.J., England, J., Gurnell, D., Jeffries, R., Shuker, L., Wharton, G., 2020. Assessing river condition: a multiscale approach designed for operational application in the context of biodiversity net gain. River Res. Appl. 36, 1559–1578. https://doi.org/10.1002/rra.3673.

Harris, I., Osborn, T.J., Jones, P., Lister, D., 2020. Version 4 of the CRU TS monthly high-resolution gridded multivariate climate dataset. Sci. Data 7, 109.

Havrdová, A., Douda, J., Doudová, J., 2023. Threats, biodiversity drivers and restoration in temperate floodplain forests related to spatial scales. Sci. Total Environ. 854, 158743. https://doi.org/10.1016/j.scitotenv.2022.158743.

Holmes, R.L., 1983. Computer-assisted quality control in tree-ring dating and measurement. Tree-Ring Bull. 43, 69–78.

Holmes, K.L., Goebel, P.C., Morris, A.E.L., 2010. Characteristics of downed wood across headwater riparian ecotones: integrating the stream with the riparian area. Can. J. For. Res. 40, 1604–1614. https://doi.org/10.1139/X10-106.

Janík, D., Adam, D., Hort, L., Král, K., Samonil, P., Unar, P., Vrška, T., 2016. Patterns of *Fraxinus angustifolia* in an alluvial old-growth forest after declines in flooding events. Eur. J. For. Res. 135, 215–228.

Janssen, P., Stella, J.C., Piégay, H., Räpple, B., Pont, B., Faton, J.M., Cornelissen, J.H.C., Evette, A., 2020. Divergence of riparian forest composition and functional traits from natural succession along a degraded river with multiple stressor legacies. Sci. Total Environ. 721, 137730.

Kibler, C.L., Schmidt, E.C., Roberts, D.A., Stella, J.C., Kui, L., Lambert, A.M., Singer, M.B., 2021. A brown wave of riparian woodland mortality following groundwater declines during the 2012–2019 California drought. Environ. Res. Lett. 16, 084030.

Klesse, S., 2021. Critical note on the application of the "two-third" spline. Dendrochronologia 65, 125786. https://doi.org/10.1016/j.dendro.2020.125786.

Lane, S.N., 2017. Natural flood management. Wiley Interdiscip. Rev. Water 4, e1211.

Le Lay, Y.-F., Piégay, H., Moulin, B., 2013. Wood entrance, deposition, transfer and effects on fluvial forms and processes: problem statements and challenging issues. Treatise Geomor. 12, 20–36.

Legendre, P., Legendre, L., 2012. Numerical Ecology. Elsevier.

Manga, M., Kirchner, J.W., 2000. Stress partitioning in streams by large woody debris. Water Resour. Res. 36, 2373–2379.

Martín, J.A., Sobrino-Plata, Rodríguez-Calcerrada, J., Collada, C., Gil, L., 2019. Breeding and scientific advances in the fight against Dutch elm disease: will they allow the use of elms in forest restoration? New For. 50, 183–215.

Maser, C., Tarrant, R.F., Trappe, J.M., Franklin, J.F., 1988. From the Forest to the Sea: A Story of Fallen Trees. USDA Forest Service, PNW Research Station General Technical Report PNW-GTR-229, Portland, Oregon, USA.

Montgomery, D.R., Collins, B.D., Buffington, J.M., Abbe, T.B., 2003. Geomorphic effects of wood in rivers. In: Gregory, S.V., Boyer, K.L., Gurnell, A.M. (Eds.), The Ecology and Management of Wood in World Rivers. American Fisheries Society Symposium, Bethesda, MD, pp. 21–47.

Mueller, J.E., 1968. An introduction to the hydraulic and topographic sinuosity indexes. Ann. Assoc. Am. Geogr. 58, 371–385.

Muller-Dombois, D., Ellenberg, H., 1974. Aims and Methods of Vegetation Ecology. John Wiley and Sons.

Nilsson, C., Riis, T., Sarneel, J.M., Svavarsdóttir, K., 2018. Ecological restoration as a means of managing inland flood hazards. BioScience 68, 89–99.

Oettel, J., Braun, M., Sallmannshofer, M., de Groot, M., Schueler, S., Virgillito, C., Westergren, M., Božič, G., Nagy, L., Stojnić, S., Lapin, K., 2022. River distance, stand basal area, and climatic conditions are the main drivers influencing lying deadwood in riparian forests. For. Ecol. Manag. 520, 120415.

Oksanen, F.J., et al., 2022. Vegan: Community Ecology Package. R package Version 2.5-7. https://CRAN.R-project.org/package=vegan.

Ollero, A., 1990. Espacios naturales de ribera en el municipio de Zaragoza. Geographicalia 27, 121–136.

Ollero, A., 2007. Channel adjustments, floodplain changes and riparian ecosystems of the middle Ebro River: assessment and management. Int. J. Water Resour. D 23, 73–90.

Phelan, C.A., Pearce, D.W., Rood, S.B., 2022. Thirsty trees: even with continuous river flow, riparian cottonwoods are constrained by water availability. Trees 36, 1247–1260.

Piégay, H., Gurnell, A.M., 1997. Large woody debris and river geomorphological pattern: examples from S.E. France and S. England. Geomorphology 19, 99–116.

Pita, P., Rodríguez-Calcerrada, J., Medel, D., Gil, L., 2018. Further insights into the components of resistance to *Ophiostoma novo-ulmi* in *Ulmus minor*: hydraulic conductance, stomatal sensitivity and bark dehydration. Tree Physiol. 38, 252–262.

Pollock, M.M., Beechie, T.J., 2014. Does riparian forest restoration thinning enhance biodiversity? The ecological importance of large wood. J. Am. Water Resour. Assoc. 50, 543–559. https://doi.org/10.1111/jawr.12206.

Polvi, L.E., Wohl, E., 2013. Biotic drivers of stream planform: implications for understanding the past and restoring the future. BioScience 63, 439–452.

R Development Core Team, 2022. R: A Language and Environment for Statistical Computing. R Foundation for Statistical Computing, Vienna, Austria. Retrieved from http://www.R-project.org/.

Rodríguez-González, P.M., Stella, J.C., Campelo, F., Ferreira, M.T., Albuquerque, A., 2010. Subsidy or stress? Tree structure and growth in wetland forests along a hydrological gradient in Southern Europe. For. Ecol. Manag. 259, 2015–2025. https://doi.org/10.1016/j.foreco.2010.02.012.

Rodríguez-González, P.M., Campelo, F., Albuquerque, A., et al., 2014. Sensitivity of black alder (*Alnus glutinosa* [L.] Gaertn.) growth to hydrological changes in wetland forests at the rear edge of the species distribution. Plant Ecol. 215, 233–245.

Rodríguez-González, P.M., Colangelo, M., Sánchez-Miranda, A., Sánchez-Salguero, R., Campelo, F., Rita, A., Gomes Marques, I., Albuquerque, A., Ripullone, F., Camarero, J.J., 2021. Climate, drought and hydrology drive narrow-leaved ash growth dynamics in southern European riparian forests. For. Ecol. Manag. 490, 119128.

Rood, S.B., Mahoney, J.M., 2023. Riparian cottonwood mortality following compound impacts from river water withdrawal and hydroclimatic variation. Ecohydrology e2550.

Ruiz-Villanueva, V., Piégay, H., Gurnell, A.M., Marston, R.A., Stoffel, M., 2016. Recent advances quantifying the large wood dynamics in river basins: new methods and remaining challenges. Rev. Geophys. 54, 611–652.

Schook, D.M., Friedman, J.M., Stricker, C.A., Csank, A.Z., Cooper, D.J., 2020. Short- and long-term responses of riparian cottonwoods (*Populus* spp.) to flow diversion: analysis of tree-ring radial growth and stable carbon isotopes. Sci. Total Environ. 735, 139523.

Schook, D.M., Friedman, J.M., Hoover, J.D., Rice, S.E., Thaxton, R.D., Cooper, D.J., 2022. Riparian forest productivity decline initiated by streamflow diversion then amplified by atmospheric drought 40 years later. Ecohydrology 15, e2408.

Sear, D.A., Millington, C.E., Kitts, D.R., Jeffries, R., 2010. Logjam controls on channel: floodplain interactions in wooded catchments and their role in the formation of multi-channel patterns. Geomorphology 116, 305–319.

Singer, M.B., Stella, J.C., Dufour, S., Piégay, H., Wilson, R.J.S., Johnstone, L., 2013. Contrasting water-uptake and growth responses to drought in co-occurring riparian tree species. Ecohydrology 6, 402–412.

Stein, E.D., Zimmerman, J., Yarnell, S.M., Stanford, B., Lane, B., Taniguchi-Quan, K.T., Obester, A., Grantham, T.E., Lusardi, R.A., Sandoval-Solis, S., 2021. The California environmental flows framework: meeting the challenges of developing a large-scale environmental flows program. Front. Environ. Sci. 9, 769943.

Stella, J.C., Bendix, J., 2019. Multiple stressors in riparian ecosystems. Multiple Stressors in River Ecosystems. Elsevier, pp. 81–110.
Stella, J.C., Riddle, J., Piégay, H., Gagnage, M., Trémélo, M.-L., 2013. Climate and local geomorphic interactions drive patterns of riparian forest decline along a Mediterranean Basin river. Geomorphology 202, 101–114.
Stromberg, J.C., Tiller, R., Richter, B., 1996. Effects of groundwater decline on riparian vegetation of semiarid regions: the San Pedro, Arizona. Ecol. Appl. 6, 113–131.
Tulik, M., Grochowina, A., Jura-Morawiec, J., Bijak, S., 2020. Groundwater level fluctuations affect the mortality of black Alder (*Alnus glutinosa* Gaertn.). Forests 11, 134.
Tyree, M.T., Kolb, K.J., Rood, S.B., Patiño, S., 1994. Vulnerability to drought-induced cavitation of riparian cottonwoods in Alberta: a possible factor in the decline of the ecosystem? Tree Physiol. 14, 455–466.
Valor, T., Camprodon, J., Buscarini, S., Casals, P., 2020. Drought-induced dieback of riparian black alder as revealed by tree rings and oxygen isotopes. For. Ecol. Manag. 478, 118500.
Van Wagner, C.E., 1968. The line intersect method for forest fuel sampling. For. Sci. 14, 20–26.
Venables, W.N., Ripley, B.D., 2002. Modern Applied Statistics with S. Springer, New York.
Wigley, T.M.L., Briffa, K.R., Jones, P.D., 1984. On the average value of correlated times series, with applications in dendroclimatology and hydrometeorology. J. Clim. Appl. Meteorol. 23, 201–213.
Williams, C.A., Cooper, D.J., 2005. Mechanisms of riparian cottomwood decline along regulated rivers. Ecosystems 8, 382–395.
Yarnell, S.M., Petts, G.E., Schmidt, J.C., Whipple, A.A., Beller, E.E., Dahm, C.N., Goodwin, P., Viers, J.H., 2015. Functional flows in modified riverscapes: hydrographs, habitats and opportunities. Bioscience 65, 963–972.